Measurement of the W mass by direct reconstruction in e^+e^- collisions at 172 GeV

R. Barate, S. Jezequel, D. Buskulic, D. Decamp, P. Ghez, C. Goy, J P. Lees, A. Lucotte, M N. Minard, J Y. Nief, et al.

EUROPEAN LABORATORY FOR PARTICLE PHYSICS (CERN)

CERN-PPE/97-164
18th December 1997

Measurement of the W Mass by Direct Reconstruction in e^+e^- Collisions at 172 GeV

The ALEPH Collaboration

Abstract

The mass of the W boson is obtained from reconstructed invariant mass distributions in W-pair events. The sample of W pairs is selected from 10.65 pb^{-1} collected with the ALEPH detector at a mean centre-of-mass energy of 172.09 GeV. The invariant mass distribution of simulated events are fitted to the experimental distributions and the following W masses are obtained:

$$\begin{aligned} \mathrm{WW} \to \mathrm{q\bar{q}q\bar{q}} \quad & m_{\mathrm{W}} = 81.30 \pm 0.47(\mathrm{stat.}) \pm 0.11(\mathrm{syst.})\ \mathrm{GeV}/c^2, \\ \mathrm{WW} \to \ell\nu\mathrm{q\bar{q}}\ (\ell = \mathrm{e}, \mu) \quad & m_{\mathrm{W}} = 80.54 \pm 0.47(\mathrm{stat.}) \pm 0.11(\mathrm{syst.})\ \mathrm{GeV}/c^2, \\ \mathrm{WW} \to \tau\nu\mathrm{q\bar{q}} \quad & m_{\mathrm{W}} = 79.56 \pm 1.08(\mathrm{stat.}) \pm 0.23(\mathrm{syst.})\ \mathrm{GeV}/c^2. \end{aligned}$$

The statistical errors are the expected errors for Monte Carlo samples of the same integrated luminosity as the data. The combination of these three measurements gives:

$$m_{\mathrm{W}} = 80.80 \pm 0.32(\mathrm{stat.}) \pm 0.11(\mathrm{syst.}) \pm 0.03(\mathrm{LEP\ energy})\ \mathrm{GeV}/c^2.$$

(*To be submitted to Phys. Lett. B.*)

The ALEPH Collaboration

R. Barate, D. Buskulic, D. Decamp, P. Ghez, C. Goy, J.-P. Lees, A. Lucotte, M.-N. Minard, J.-Y. Nief, B. Pietrzyk

Laboratoire de Physique des Particules (LAPP), IN^{2}P^3-CNRS, 74019 Annecy-le-Vieux Cedex, France

G. Boix, M.P. Casado, M. Chmeissani, J.M. Crespo, M. Delfino, E. Fernandez, M. Fernandez-Bosman, Ll. Garrido,[15] E. Graugès, A. Juste, M. Martinez, G. Merino, R. Miquel, Ll.M. Mir, P. Morawitz, I.C. Park, A. Pascual, J.A. Perlas, I. Riu, F. Sanchez

Institut de Física d'Altes Energies, Universitat Autònoma de Barcelona, 08193 Bellaterra (Barcelona), Spain[7]

A. Colaleo, D. Creanza, M. de Palma, G. Gelao, G. Iaselli, G. Maggi, M. Maggi, S. Nuzzo, A. Ranieri, G. Raso, F. Ruggieri, G. Selvaggi, L. Silvestris, P. Tempesta, A. Tricomi,[3] G. Zito

Dipartimento di Fisica, INFN Sezione di Bari, 70126 Bari, Italy

X. Huang, J. Lin, Q. Ouyang, T. Wang, Y. Xie, R. Xu, S. Xue, J. Zhang, L. Zhang, W. Zhao

Institute of High-Energy Physics, Academia Sinica, Beijing, The People's Republic of China[8]

D. Abbaneo, R. Alemany, U. Becker, P. Bright-Thomas, D. Casper, M. Cattaneo, F. Cerutti, V. Ciulli, G. Dissertori, H. Drevermann, R.W. Forty, M. Frank, F. Gianotti, R. Hagelberg, J.B. Hansen, J. Harvey, P. Janot, B. Jost, I. Lehraus, P. Mato, A. Minten, L. Moneta,[22] A. Pacheco, J.-F. Pusztaszeri,[20] F. Ranjard, L. Rolandi, D. Rousseau, D. Schlatter, M. Schmitt, O. Schneider, W. Tejessy, F. Teubert, I.R. Tomalin, M. Vreeswijk, H. Wachsmuth, A. Wagner[1]

European Laboratory for Particle Physics (CERN), 1211 Geneva 23, Switzerland

Z. Ajaltouni, F. Badaud G. Chazelle, O. Deschamps, A. Falvard, C. Ferdi, P. Gay, C. Guicheney, P. Henrard, J. Jousset, B. Michel, S. Monteil, J-C. Montret, D. Pallin, P. Perret, F. Podlyski, J. Proriol, P. Rosnet

Laboratoire de Physique Corpusculaire, Université Blaise Pascal, IN^{2}P^3-CNRS, Clermont-Ferrand, 63177 Aubière, France

T. Fearnley, J.D. Hansen, J.R. Hansen, P.H. Hansen, B.S. Nilsson, B. Rensch, A. Wäänänen

Niels Bohr Institute, 2100 Copenhagen, Denmark[9]

G. Daskalakis, A. Kyriakis, C. Markou, E. Simopoulou, A. Vayaki

Nuclear Research Center Demokritos (NRCD), Athens, Greece

A. Blondel, J.-C. Brient, F. Machefert, A. Rougé, M. Rumpf, A. Valassi,[6] H. Videau

Laboratoire de Physique Nucléaire et des Hautes Energies, Ecole Polytechnique, IN^{2}P^3-CNRS, 91128 Palaiseau Cedex, France

T. Boccali, E. Focardi, G. Parrini, K. Zachariadou

Dipartimento di Fisica, Università di Firenze, INFN Sezione di Firenze, 50125 Firenze, Italy

R. Cavanaugh, M. Corden, C. Georgiopoulos, T. Huehn, D.E. Jaffe

Supercomputer Computations Research Institute, Florida State University, Tallahassee, FL 32306-4052, USA [13,14]

A. Antonelli, G. Bencivenni, G. Bologna,[4] F. Bossi, P. Campana, G. Capon, V. Chiarella, G. Felici, P. Laurelli, G. Mannocchi,[5] F. Murtas, G.P. Murtas, L. Passalacqua, M. Pepe-Altarelli

Laboratori Nazionali dell'INFN (LNF-INFN), 00044 Frascati, Italy

L. Curtis, S.J. Dorris, A.W. Halley, J.G. Lynch, P. Negus, V. O'Shea, C. Raine, J.M. Scarr, K. Smith, P. Teixeira-Dias, A.S. Thompson, E. Thomson, F. Thomson, J.J. Ward

Department of Physics and Astronomy, University of Glasgow, Glasgow G12 8QQ,United Kingdom[10]

O. Buchmüller, S. Dhamotharan, C. Geweniger, G. Graefe, P. Hanke, G. Hansper, V. Hepp, E.E. Kluge,

A. Putzer, J. Sommer, K. Tittel, S. Werner, M. Wunsch

Institut für Hochenergiephysik, Universität Heidelberg, 69120 Heidelberg, Fed. Rep. of Germany[16]

R. Beuselinck, D.M. Binnie, W. Cameron, P.J. Dornan, M. Girone, S. Goodsir, E.B. Martin, N. Marinelli, A. Moutoussi, J. Nash, J.K. Sedgbeer, P. Spagnolo, M.D. Williams

Department of Physics, Imperial College, London SW7 2BZ, United Kingdom[10]

V.M. Ghete, P. Girtler, E. Kneringer, D. Kuhn, G. Rudolph

Institut für Experimentalphysik, Universität Innsbruck, 6020 Innsbruck, Austria[18]

A.P. Betteridge, C.K. Bowdery, P.G. Buck, P. Colrain, G. Crawford, A.J. Finch, F. Foster, G. Hughes, R.W.L. Jones, E.P. Whelan, M.I. Williams

Department of Physics, University of Lancaster, Lancaster LA1 4YB, United Kingdom[10]

I. Giehl, C. Hoffmann, K. Jakobs, K. Kleinknecht, G. Quast, B. Renk, E. Rohne, H.-G. Sander, P. van Gemmeren, C. Zeitnitz

Institut für Physik, Universität Mainz, 55099 Mainz, Fed. Rep. of Germany[16]

J.J. Aubert, C. Benchouk, A. Bonissent, G. Bujosa, J. Carr, P. Coyle, A. Ealet, D. Fouchez, O. Leroy, F. Motsch, P. Payre, M. Talby, A. Sadouki, M. Thulasidas, A. Tilquin, K. Trabelsi

Centre de Physique des Particules, Faculté des Sciences de Luminy, IN^{2}P^3-CNRS, 13288 Marseille, France

M. Aleppo, M. Antonelli, F. Ragusa

Dipartimento di Fisica, Università di Milano e INFN Sezione di Milano, 20133 Milano, Italy.

R. Berlich, W. Blum, V. Büscher, H. Dietl, G. Ganis, C. Gotzhein, H. Kroha, G. Lütjens, G. Lutz, C. Mannert, W. Männer, H.-G. Moser, R. Richter, A. Rosado-Schlosser, S. Schael, R. Settles, H. Seywerd, H. Stenzel, W. Wiedenmann, G. Wolf

Max-Planck-Institut für Physik, Werner-Heisenberg-Institut, 80805 München, Fed. Rep. of Germany[16]

J. Boucrot, O. Callot,[12] S. Chen, M. Davier, L. Duflot, J.-F. Grivaz, Ph. Heusse, A. Höcker, A. Jacholkowska, M.M. Kado, D.W. Kim,[2] F. Le Diberder, J. Lefrançois, A.-M. Lutz, M.-H. Schune, L. Serin, E. Tournefier, J.-J. Veillet, I. Videau, D. Zerwas

Laboratoire de l'Accélérateur Linéaire, Université de Paris-Sud, IN^{2}P^3-CNRS, 91405 Orsay Cedex, France

P. Azzurri, G. Bagliesi,[12] S. Bettarini, C. Bozzi, G. Calderini, R. Dell'Orso, R. Fantechi, I. Ferrante, A. Giassi, A. Gregorio, F. Ligabue, A. Lusiani, P.S. Marrocchesi, A. Messineo, F. Palla, G. Rizzo, G. Sanguinetti, A. Sciabà, G. Sguazzoni, J. Steinberger, R. Tenchini, C. Vannini, A. Venturi, P.G. Verdini

Dipartimento di Fisica dell'Università, INFN Sezione di Pisa, e Scuola Normale Superiore, 56010 Pisa, Italy

G.A. Blair, L.M. Bryant, J.T. Chambers, J. Coles, M.G. Green, T. Medcalf, P. Perrodo, J.A. Strong, J.H. von Wimmersperg-Toeller

Department of Physics, Royal Holloway & Bedford New College, University of London, Surrey TW20 OEX, United Kingdom[10]

D.R. Botterill, R.W. Clifft, T.R. Edgecock, S. Haywood, P. Maley, P.R. Norton, J.C. Thompson, A.E. Wright

Particle Physics Dept., Rutherford Appleton Laboratory, Chilton, Didcot, Oxon OX11 OQX, United Kingdom[10]

B. Bloch-Devaux, P. Colas, B. Fabbro, G. Faïf, E. Lançon, M.-C. Lemaire, E. Locci, P. Perez, H. Przysiezniak, J. Rander, J.-F. Renardy, A. Rosowsky, A. Roussarie, A. Trabelsi, B. Vallage

CEA, DAPNIA/Service de Physique des Particules, CE-Saclay, 91191 Gif-sur-Yvette Cedex, France[17]

S.N. Black, J.H. Dann, H.Y. Kim, N. Konstantinidis, A.M. Litke, M.A. McNeil, G. Taylor

Institute for Particle Physics, University of California at Santa Cruz, Santa Cruz, CA 95064, USA[19]

C.N. Booth, C.A.J. Brew, S. Cartwright, F. Combley, M.S. Kelly, M. Lehto, J. Reeve, L.F. Thompson
Department of Physics, University of Sheffield, Sheffield S3 7RH, United Kingdom[10]

K. Affholderbach, A. Böhrer, S. Brandt, G. Cowan, J. Foss, C. Grupen, L. Smolik, F. Stephan
Fachbereich Physik, Universität Siegen, 57068 Siegen, Fed. Rep. of Germany[16]

M. Apollonio, L. Bosisio, R. Della Marina, G. Giannini, B. Gobbo, G. Musolino
Dipartimento di Fisica, Università di Trieste e INFN Sezione di Trieste, 34127 Trieste, Italy

J. Putz, J. Rothberg, S. Wasserbaech, R.W. Williams
Experimental Elementary Particle Physics, University of Washington, WA 98195 Seattle, U.S.A.

S.R. Armstrong, E. Charles, P. Elmer, D.P.S. Ferguson, Y. Gao, S. González, T.C. Greening, O.J. Hayes, H. Hu, S. Jin, P.A. McNamara III, J.M. Nachtman,[21] J. Nielsen, W. Orejudos, Y.B. Pan, Y. Saadi, I.J. Scott, J. Walsh, Sau Lan Wu, X. Wu, J.M. Yamartino, G. Zobernig
Department of Physics, University of Wisconsin, Madison, WI 53706, USA[11]

[1]Now at Schweizerischer Bankverein, Basel, Switzerland.
[2]Permanent address: Kangnung National University, Kangnung, Korea.
[3]Also at Dipartimento di Fisica, INFN Sezione di Catania, Catania, Italy.
[4]Also Istituto di Fisica Generale, Università di Torino, Torino, Italy.
[5]Also Istituto di Cosmo-Geofisica del C.N.R., Torino, Italy.
[6]Supported by the Commission of the European Communities, contract ERBCHBICT941234.
[7]Supported by CICYT, Spain.
[8]Supported by the National Science Foundation of China.
[9]Supported by the Danish Natural Science Research Council.
[10]Supported by the UK Particle Physics and Astronomy Research Council.
[11]Supported by the US Department of Energy, grant DE-FG0295-ER40896.
[12]Also at CERN, 1211 Geneva 23,Switzerland.
[13]Supported by the US Department of Energy, contract DE-FG05-92ER40742.
[14]Supported by the US Department of Energy, contract DE-FC05-85ER250000.
[15]Permanent address: Universitat de Barcelona, 08208 Barcelona, Spain.
[16]Supported by the Bundesministerium für Bildung, Wissenschaft, Forschung und Technologie, Fed. Rep. of Germany.
[17]Supported by the Direction des Sciences de la Matière, C.E.A.
[18]Supported by Fonds zur Förderung der wissenschaftlichen Forschung, Austria.
[19]Supported by the US Department of Energy, grant DE-FG03-92ER40689.
[20]Now at School of Operations Research and Industrial Engireering, Cornell University, Ithaca, NY 14853-3801, U.S.A.
[21]Now at University of California at Los Angeles (UCLA), Los Angeles, CA 90024, U.S.A.
[22]Now at University of Geneva, 1211 Geneva 4, Switzerland.

1 Introduction

Pairs of W bosons have been produced at LEP since June 1996, when the centre-of-mass energy of the colliding beams reached the W-pair threshold of 161 GeV. At this energy, first measurements of the W mass at LEP were made using the measured cross sections [1, 2]. A larger sample of W pairs was obtained when running at 172 GeV during October-November 1996, allowing the W mass to be measured from the direct reconstruction of the invariant mass of its decay products. Studies of W bosons have taken place in $\mathrm{p\bar{p}}$ collisions, where large samples of single W's decaying into $\mathrm{e}\nu_{\mathrm{e}}$ and $\mu\nu_{\mu}$ have been used to measure the W mass [3]. Combining the hadron collider results, the precision on the value for m_{W} is 90 MeV/c^2 [4]. The comparison of this measurement with the prediction based on the Z mass and the Fermi constant constitutes a sensitive probe of electroweak radiative corrections. Combined with the present precision on the top quark mass [5], a precise W mass measurement can either improve the constraints on the mass of the undiscovered Higgs boson obtained from electroweak fits, or could reveal new physics.

Unlike at $\mathrm{p\bar{p}}$ colliders, W's can be detected in all decay modes at LEP2, and the centre-of-mass energy is known precisely. Thus, energy and momentum conservation constraints can be applied to the event reconstruction, leading to a much improved invariant mass resolution. This is true both in semileptonic W pairs, where one W boson decays into two hadronic jets and the other into a lepton and a neutrino, and in W pairs decaying into four jets where the relatively poor jet energy resolution is compensated by these kinematic constraints. The purely leptonic double decays are not used in the measurement described here.

This letter presents a first ALEPH measurement of the W mass by direct reconstruction. An integrated luminosity of 10.65 ± 0.08 pb^{-1} was recorded, at a mean centre-of-mass energy of 172.09 ± 0.06 GeV [6]: 1.11 pb^{-1} at 170.28 GeV and 9.54 pb^{-1} at 172.30 GeV. The letter is organised as follows: first, the important properties of the ALEPH detector for this analysis are recalled and a description is given of the Monte Carlo event generators for the processes involved. Event selection and mass reconstruction for the different channels are then described, followed by the technique in which the invariant mass distributions of reweighted Monte Carlo events are fitted to the data distributions to extract the W mass for the purely hadronic and semileptonic channels separately. Stability checks of the measurement and a study of systematic errors are then presented. Finally, the measurements of the W mass in each channel are combined, taking into account common sources of systematic errors.

2 The ALEPH detector

A detailed description of the ALEPH detector can be found in Ref. [7] and of its performance in Ref. [8]. Charged particles are detected in the central part of the detector. From the beam crossing point outwards, a silicon vertex detector, a cylindrical drift chamber, and a large time projection chamber (TPC) measure up to 31 coordinates along the charged particle trajectories. A 1.5 T axial magnetic field is provided by a superconducting solenoidal coil. A resolution of $\delta p_T/p_T = 6 \cdot 10^{-4} p_T \oplus 0.005$ (p_T in GeV/c) can be achieved. Hereafter, charged particle tracks reconstructed from at least

four hits in the TPC and originating from within a cylinder of 2 cm radius and 20 cm length, centred on the nominal interaction point and parallel to the beam axis, are called *good tracks*.

Electrons and photons are identified in the electromagnetic calorimeter by their characteristic longitudinal and transverse shower development. The calorimeter, a lead/wire-plane sampling device with fine readout segmentation and total thickness of 22 radiation lengths at normal incidence, provides a relative energy resolution of $0.180/\sqrt{E}+0.009$ (E in GeV).

Muons are identified by their penetration pattern in the hadron calorimeter, a 1.2 m thick iron yoke instrumented with 23 layers of streamer tubes, together with two surrounding layers of muon chambers. In association with the electromagnetic calorimeter, the hadron calorimeter also provides a measurement of the energy of charged and neutral hadrons with a relative resolution of $0.85/\sqrt{E}$ (E in GeV).

The total visible energy and momentum, and also the missing energy, are evaluated by an energy flow reconstruction algorithm [8] which combines all of the above measurements, supplemented at low polar angles by the energy detected in the luminosity calorimeters. The algorithm also provides a list of charged and neutral reconstructed objects, called *energy flow objects*, from which jets are reconstructed with a typical angular resolution of 30 mrad in space. The jet energy resolution is approximately given by $\sigma_E = (0.6\sqrt{E}+0.6)\mathrm{GeV}\cdot(1+\cos^2\theta)$, where E (in GeV) and θ are the jet energy and polar angle. The jet energy and angular resolution as well as calibrations were obtained from extensive studies of $Z \to \mathrm{q\bar{q}}$ events both in data and Monte Carlo. Discrepancies between data and simulation were used in evaluating systematic errors.

3 Monte Carlo samples

The W mass is extracted by comparing the experimental distributions to the corresponding Monte Carlo distributions, where generated events are processed through a full simulation of the ALEPH detector response and through the same reconstruction chain. Two Monte Carlo event generators are used to simulate the signal events, i.e. four-fermion final states which can come from WW production and decay:

- `KORALW`, version 1.21 [9]. This program includes multi-photon initial state radiation (ISR) with finite photon transverse momentum via Yennie-Frautschi-Suura exponentiation [10], final state radiation via `PHOTOS` [11], and Coulomb correction [12]. It can generate CC03 diagrams, which correspond to the three Feynman diagrams that contribute to the production of two resonant W's at tree level, or include four-fermion diagrams computed with the `GRACE` package [13], with fixed W and Z widths. The `JETSET` [14] package takes care of gluon radiation and hadronisation. In four-quark final states, the colour flow between fermions is chosen with probabilities proportional to the matrix elements squared for WW and ZZ production [15]. Colour flow between two fermions produced by two different bosons, known as colour reconnection [16, 17], is not included. Samples of 100,000 events were generated with W masses of 79.25, 80.25 and 81.25 GeV/c^2, for all four-fermion diagrams. Loose cuts were applied at the generation level on the outgoing electron angle or the fermion-antifermion pair invariant masses, avoiding regions of phase space with poles in the cross section. Signal events produced in these regions

would in any case be rejected by the selection cuts. Seven additional samples of 20,000 events each were generated with W masses of 79.25, 79.75, 80.00, 80.25, 80.50, 80.75 and 81.25 GeV/c^2 for all four-fermion diagrams.

- For comparison, the EXCALIBUR [18] generator is also used. It includes ISR collinear with the beams [19], final state radiation via PHOTOS [11], Coulomb correction [12] and hadronisation by JETSET [14]. A sample was generated with $m_{\mathrm{W}} = 80.25$ GeV/c^2 and the same choice of colour flow with loose cuts applied at the generation level as above. For colour reconnection studies the same events were hadronised following the ansatz of [16].

Monte Carlo samples, with integrated luminosities corresponding to at least twenty times that of the data, were fully simulated for all background reactions. Annihilation into quark pairs, $\mathrm{e^+e^-} \to \mathrm{q\bar{q}}(\gamma)$, was simulated with PYTHIA [14]. Two-photon ($\gamma\gamma$) reactions into leptons and hadrons were simulated with the PHOT02 [20] and PYTHIA generators. KORALZ [21] and UNIBAB [22] were used for dilepton final states. Finally, PYTHIA and FERMISV [23] were used for various processes leading to four-fermion final states. Where appropriate, results from the two programs are cross-checked against each other. Some four-fermion configurations are found in both the signal WW and background ZZ Monte Carlo's. Hence, events with a flavour content that could originate from WW production are explicitly rejected from the ZZ sample.

4 Event selections

In the following sections, the event selections are described for the three types of events considered: $\mathrm{W^+W^-} \to \mathrm{q\bar{q}q\bar{q}}$, $\mathrm{W^+W^-} \to \mathrm{e}(\mu)\nu\mathrm{q\bar{q}}$ and $\mathrm{WW} \to \tau\nu\mathrm{q\bar{q}}$. Using a Monte Carlo sample generated at $m_{\mathrm{W}} = 80.25$ GeV/c^2, the expected observable cross sections for each type together with their corresponding backgrounds are summarised in Table 1. They are calculated from the numbers of events surviving the selection cuts described below and the mass reconstruction procedures described in Section 5. The selection efficiencies and purities were also determined for other m_{W} values and their dependence on the W mass is negligible (see Section 8.4).

4.1 $\mathrm{W^+W^-} \to \mathrm{q\bar{q}q\bar{q}}$ events

At $\sqrt{s} = 172$ GeV the main source of background to the $\mathrm{e^+e^-} \to \mathrm{WW} \to \mathrm{q\bar{q}q\bar{q}}$ process (denoted 4q) is $\mathrm{e^+e^-} \to \mathrm{q\bar{q}}$ production, followed by the $\mathrm{e^+e^-} \to \mathrm{ZZ}$ and $\mathrm{e^+e^-} \to \mathrm{WW} \to q\bar{q}\ell\nu$ processes. To select WW hadronic decays, the following cuts are applied in the preselection: the missing energy must be smaller than 40 GeV, the number of energy flow objects larger than 45, and the number of jets found with the JADE algorithm [24] with $y_{\mathrm{cut}} = 0.005$ larger than three. The events are then forced into four jets using the DURHAM-P algorithm (see Section 5.1). Further preselection cuts are applied to these DURHAM jets: more than one good track inside a jet, and the fraction of electromagnetic to total energy in a jet less than 0.9.

A feed-forward neural network with 21 input variables is then used to tag the signal events. The most discriminating variables are found to be the sum of cosines of the angles between the jets, the Fox-Wolfram moments, the largest of the minimum invariant masses

Table 1: Cross sections of various processes after analysis cuts. The quoted efficiencies are relative to the predicted number of events for each channel in the KORALW four-fermion (4f) Monte Carlo with $m_{\mathrm{W}} = 80.25$ GeV/c^2. For the 4q channel, only WW $\to$ 4q events which have passed the analysis cuts are considered as signal. For the semileptonic channels, all WW events which have passed the analysis cuts are considered as signal. (This includes τ events in the eμ sample and vice versa.)

	σ_{cuts} (pb)		
Process	4q sel.	eμ sel.	τ sel.
WW $\to$ q$\bar{\mathrm{q}}$q$\bar{\mathrm{q}}$	4.43	0.00	0.01
WW $\to$ e(μ)νq$\bar{\mathrm{q}}$	0.02	3.08	0.12
WW $\to \tau\nu$q$\bar{\mathrm{q}}$	0.01	0.16	0.83
WW $\to \ell\nu\ell\nu$	0.00	0.00	0.00
q$\bar{\mathrm{q}}(\gamma)$	1.02	0.03	0.06
ZZ	0.08	0.02	0.00
Weν	0.00	0.01	0.00
Zee	0.01	0.02	0.00
$\tau\tau$	0.00	0.01	0.00
2-photon	0.00	0.00	0.00
Efficiency (4f) (%)	76.9	93.6	50.5
Purity (4f) (%)	79.5	97.7	94.0

from each of the three $\mathrm{W^+W^-}$ di-jet combinations, and the maximum invariant mass of all six di-jet combinations. A description of the neural network and the variables it uses, as well as the distribution of the neural network output, are given in [25]. To select W hadronic events, the neural network output is required to be larger than -0.3. Monte Carlo studies confirm that the fitted W mass is stable as a function of the cut value. After all analysis cuts, 65 events are selected. Monte Carlo studies predict 59.3 events (47.2 signal events and 12.1 background events).

4.2 $\mathbf{W^+W^- \to e\nu q\bar{q}}$ and $\mathbf{W^+W^- \to \mu\nu q\bar{q}}$ events

The characteristic features of $\mathrm{W^+W^-} \to \mathrm{e}(\mu)\nu\mathrm{q\bar{q}}$ events (denoted eμ) are a high energy isolated lepton and a large amount of missing energy due to the neutrino, along with two or more jets.

The selection requires at least five good tracks with a total charged energy greater than $0.10\sqrt{s}$. The magnitude and direction of the missing momentum vector is used to discriminate between the signal process and the q$\bar{\mathrm{q}}$ background, eliminating those radiative returns in which the high-energy photon escapes down the beam pipe and the non-radiative events which are fully contained within the detector. The charged track with the highest momentum component antiparallel to the missing momentum is chosen as the lepton candidate. Loose electron or muon identification criteria and an energy of at least 15 GeV are required for the lepton candidate.

After this preselection, the probability for an event to come from the signal process is determined using the energy of the lepton, the total missing transverse momentum and the lepton isolation. The procedure is described in [1]. Events are selected if they have a probability larger than 0.36 to be an eνq$\bar{\mathrm{q}}$ event or a probability larger than 0.70 to be

a $\mu\nu q\bar{q}$ event. These cut values are determined using Monte Carlo, where the expected error on the W mass is minimised. After all analysis cuts, 34 events remain: 14 in the electron channel and 20 in the muon channel. Monte Carlo studies predict 34.7 (33.9 signal and 0.8 background) events.

In the case of candidate $e\nu q\bar{q}$ events, the energy of the electron is corrected if evidence for a bremsstrahlung photon is found, either in the form of a separate cluster in the electromagnetic calorimeter or as an excess of energy in the electron cluster. This excess is determined as in [26].

4.3 $WW \to \tau\nu q\bar{q}$ events

The $WW \to \tau\nu q\bar{q}$ (denoted τ) event selection cuts are described elsewhere [1, 27]. In summary, an event is selected if it passes a series of preselection cuts and if it satisfies either a topological or a global selection. It must also not pass the $e\mu$ selection, so that the two samples are independent. Unlike the cross section analysis [27], a τ jet is always searched for, and is required for the measurement of the W mass; these represent 90% of the events selected as in [27]. After all analysis cuts, 10 events remain. Monte Carlo studies predict 11.3 events (10.7 signal and 0.6 background).

5 Invariant mass reconstruction

Following the event selection, the determination of the invariant mass of the W candidates in each event requires several steps. The jet finding is discussed first, followed by the invariant mass reconstruction method via a kinematic fit. Finally the jet pairing method, which concerns only the 4q channel, is described.

5.1 Jet clustering algorithm

The `DURHAM` [28] algorithm is used to cluster the energy flow objects into jets in a massless combination (denoted as the `P` scheme) of the particles. Monte Carlo studies show that for the 4q channel, this `DURHAM-P` scheme is the most successful jet clustering algorithm for associating particle momenta correctly to their parent W bosons. However, to reduce bias in the reconstructed invariant masses, the jet four-momenta are built from the sum of the particle four-momenta, taking the particle masses into account. Using this procedure, known as the `DURHAM-PE` scheme, the 4q events are forced into four jets. In the case of semileptonic events, this procedure is applied to all energy flow objects that are not used to construct the lepton, and these are forced into two jets.

5.2 Kinematic fit

In order to improve the mass resolution a kinematic fit is applied to the four reconstructed objects (where *object* here refers to jets, leptons or to the missing momentum vector). Average corrections are first applied to the object momenta and polar angles to take into account loss of particles in the regions of the detector close to the beam axis. In the fit, the measured momenta $\vec{p}_i^{\,\mathrm{m}}$ of the four objects are modified to produce the corrected momenta $\vec{p}_i^{\,\mathrm{corr}} = a_i\vec{p}_i^{\,\mathrm{m}} + b_i\vec{u}_i^{\,b} + c_i\vec{u}_i^{\,c}$, where a_i, b_i and c_i are the parameters of the fit.

The unit vectors $\vec{u}_i{}^b$ and $\vec{u}_i{}^c$ are perpendicular to the measured object axis, where $\vec{u}_i{}^b$ is in the plane defined by the object axis and the z axis, and $\vec{u}_i{}^c$ is perpendicular to $\vec{u}_i{}^b$. The input errors on a_i, b_i and c_i are determined from Monte Carlo assuming the parameters have Gaussian distributions. Both the parameter values and their errors depend on the type of object, its energy and direction. The energies of jets are assumed to scale in the ratio of their fitted to reconstructed momenta. For τ events, the detected decay products of each τ are used to determine its most likely momentum and direction in the fit. For all semileptonic events, the candidate neutrino from the W decay is assigned the missing momentum and a zero mass. A χ^2 is then constructed with these parameters and the constraints are imposed by Lagrange multipliers. The minimisation of this χ^2 is done via an iterative procedure.

Imposing energy and momentum conservation alone corresponds to a four-constraint (4C) fit giving two different masses for the candidate W bosons. The results of the 4C fit can be further improved by building a new observable from the fitted mass and energy of each W, the rescaled mass:

$$m_{ij}^{\mathrm{resc}} = m_{ij}\frac{E_b}{E_i + E_j} \ ,$$

where E_b is the beam energy and E_i, E_j are the object energies. The rescaled masses are directly related to the velocities of the two W's, and each one depends on the mass of both W's. Use of the rescaled 4C masses results in a large cancellation of the pure 4C measurement errors, in particular those coming from misassignment of energy from one W to the other. In the case of the hadronic events, the 4C fit with rescaling is chosen.

For the semileptonic events, the fit is improved by imposing equal masses as well as energy and momentum conservation. This effectively becomes a 2C fit since the three-momentum of the neutrino is not directly measured.

5.3 Jet pairing for $\mathbf{W^+W^- \to q\bar{q}q\bar{q}}$ events

For selected hadronic events, the four jets are coupled into two di-jets in three different ways. For each combination, two rescaled 4C masses are determined. A jet pairing algorithm which selects just one of the combinations is used. It chooses the one for which the difference between the two masses is the smallest, unless this combination has the smallest sum of the two di-jet opening angles (the opening angle is the angle between the two jets of a candidate W); in this case, the combination with the second smallest mass difference is selected. For the chosen combination, the two masses m_1 and m_2 are treated separately. The order of these two masses is taken randomly, so that the expected distribution for both masses is exactly the same. Both masses must satisfy $50 < m_i < 86$ GeV/c^2 and at least one of the two masses must satisfy $74 < m_i < 86$ GeV/c^2.

6 Extraction of the W mass

To extract the W boson mass, the invariant mass distribution of reweighted Monte Carlo events is fitted to the data events distribution, after the selection and mass reconstruction steps. The fitting method and the results are described in the following sections.

6.1 Fitting technique

The invariant mass distributions have a Breit-Wigner like shape which is distorted by ISR, phase space boundary, detector resolution, misassignment of particles between W's, background contamination and event selection. To take into account all these effects, the measured invariant mass distributions are compared with the corresponding Monte Carlo distributions generated with different input W masses. A binned log-likelihood function is used to extract the value of m_{W} which best fits the data. The W width is given the Standard Model value for a given W mass. For $m_{\mathrm{W}} = 80.25$ GeV/c^2, it is set to $\Gamma_{\mathrm{W}} = 2.08$ GeV.

To avoid having to generate large Monte Carlo samples at many different input W masses, a Monte Carlo event reweighting technique is used. Large samples were generated for all four-fermion diagrams and constant width at three input masses $m_{\mathrm{W}}^{\mathrm{MC}} = 79.25,\ 80.25$ and 81.25 GeV/c^2. These Monte Carlo events are reweighted using the ratio of squared matrix elements:

$$w_i(m_{\mathrm{W}}, \Gamma_{\mathrm{W}}) = \frac{\mid \mathcal{M}(m_{\mathrm{W}}, \Gamma_{\mathrm{W}}, p_i^1, p_i^2, p_i^3, p_i^4) \mid^2}{\mid \mathcal{M}(m_{\mathrm{W}}^{\mathrm{MC}}, \Gamma_{\mathrm{W}}^{\mathrm{MC}}, p_i^1, p_i^2, p_i^3, p_i^4) \mid^2} \ ,$$

where p_i^j denotes the four-momentum of the jth outgoing fermion for a particular event i, Γ_{W} is the W width, and $\mathcal{M}(m_{\mathrm{W}}, \Gamma_{\mathrm{W}}, p_i^1, p_i^2, p_i^3, p_i^4)$ is the matrix element of the process $\mathrm{e^+e^-} \to \mathrm{W^+W^-} \to \mathrm{f_1\bar{f}_2f_3\bar{f}_4}$. The matrix element is evaluated for the CC03 diagrams.

The background Monte Carlo samples are also used in the fit such that the background cross section is fixed. The signal selection efficiency is assumed to be constant with m_{W}, hence the signal purity varies only due to the W-pair cross section dependence on m_{W}. The resulting invariant mass distribution is fitted to the data using the three WW reference Monte Carlo samples. The final data result is obtained using the reference sample with the input mass which is closest to the fitted data mass. The fit is performed in the 74-86 GeV/c^2 mass range, which is chosen following Monte Carlo studies. These show that the reweighted Monte Carlo fitting technique has maximal sensitivity to the shape of the invariant mass distribution in this mass range. Negligible information about the input W mass can be extracted from the reduced statistics data below this mass range.

When the Z mass was measured at LEP1, a mass definition corresponding to a propagator including an s-dependent width was used, whereas in the formulae and Monte Carlo used to extract the W mass, a Breit-Wigner propagator with fixed width is used, as suggested in Ref. [29]. To make both measurements consistent with each other, a positive shift of 27 MeV/c^2 is applied throughout on the measured W mass.

6.2 The results

For the events selected, the fit results are: $m_1 = 81.43^{+0.52}_{-0.53}$ GeV/c^2 and $m_2 = 81.16^{+0.56}_{-0.62}$ GeV/c^2 for the two rescaled masses in the 4q channel, $m_{\mathrm{W}} = 80.54 \pm 0.37$ GeV/c^2 for the eμ events and $m_{\mathrm{W}} = 79.56 \pm 1.94$ GeV/c^2 for the τ events. For the hadronic channel, the event-by-event correlation between the two rescaled masses is $63.5 \pm 7.4\%$, in good agreement with the Monte Carlo expectation of $66.7 \pm 0.3\%$.

Due to the small size of the data samples, the statistical errors resulting from the fits have a large uncertainty. For each selection, a large number of Monte Carlo subsamples are studied, each with the same integrated luminosity as the data, such that they contain the

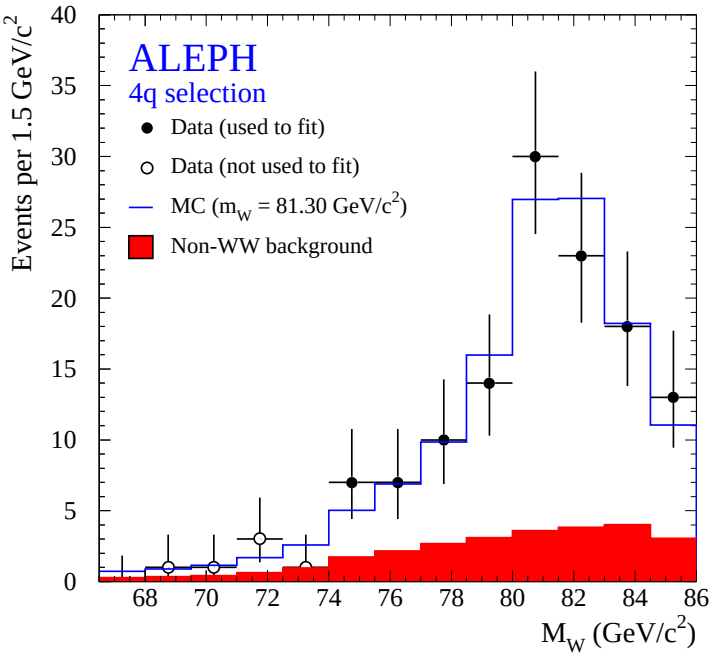

Figure 1: Mass distribution (m_1 and m_2 combined) for hadronic data (points with error bars), background Monte Carlo (shaded area) and signal+background Monte Carlo for the best fit to the data (solid line histogram).

expected number of events for the different selections. The widths of the pull distributions, where the pull is defined as $(m_{\mathrm{W}}^{\mathrm{fit}} - m_{\mathrm{W}}^{\mathrm{MC}})/\sigma^{\mathrm{fit}}$, are consistent with unity as a function of the fit error, confirming the reliability of the fit errors. The mean value of the fit error distributions for these Monte Carlo subsamples is taken as the expected error. These are 0.58 GeV/c^2 for each of the two hadronic masses, 0.47 GeV/c^2 for the eμ events and 1.08 GeV/c^2 for the τ events. Both the fit errors and the expected errors are reliable estimates of the W mass error. However, since the expected errors are determined with better precision, they are quoted as the final statistical errors.

For the hadronic events, the expected correlation between the fitted masses extracted from the two rescaled mass distributions is computed using the Monte Carlo subsamples. The correlation value is $33.2 \pm 5.1\%$, independent of the W mass. The combined result for the 4q channel, using the Monte Carlo expected errors and correlation gives:

$$\mathrm{4q}: \quad m_{\mathrm{W}} = 81.30 \pm 0.47 \ \ \mathrm{GeV}/c^2.$$

For the eμ and τ channels, the results quoting the expected errors are:

$$\mathrm{e}\mu: \quad m_{\mathrm{W}} = 80.54 \pm 0.47 \ \ \mathrm{GeV}/c^2$$
$$\tau: \quad m_{\mathrm{W}} = 79.56 \pm 1.08 \ \ \mathrm{GeV}/c^2.$$

Figures 1 and 2 show the mass distributions for the selected events in each channel.

7 Consistency and stability checks

The following checks are made to confirm the consistency and stability of the method and its results.

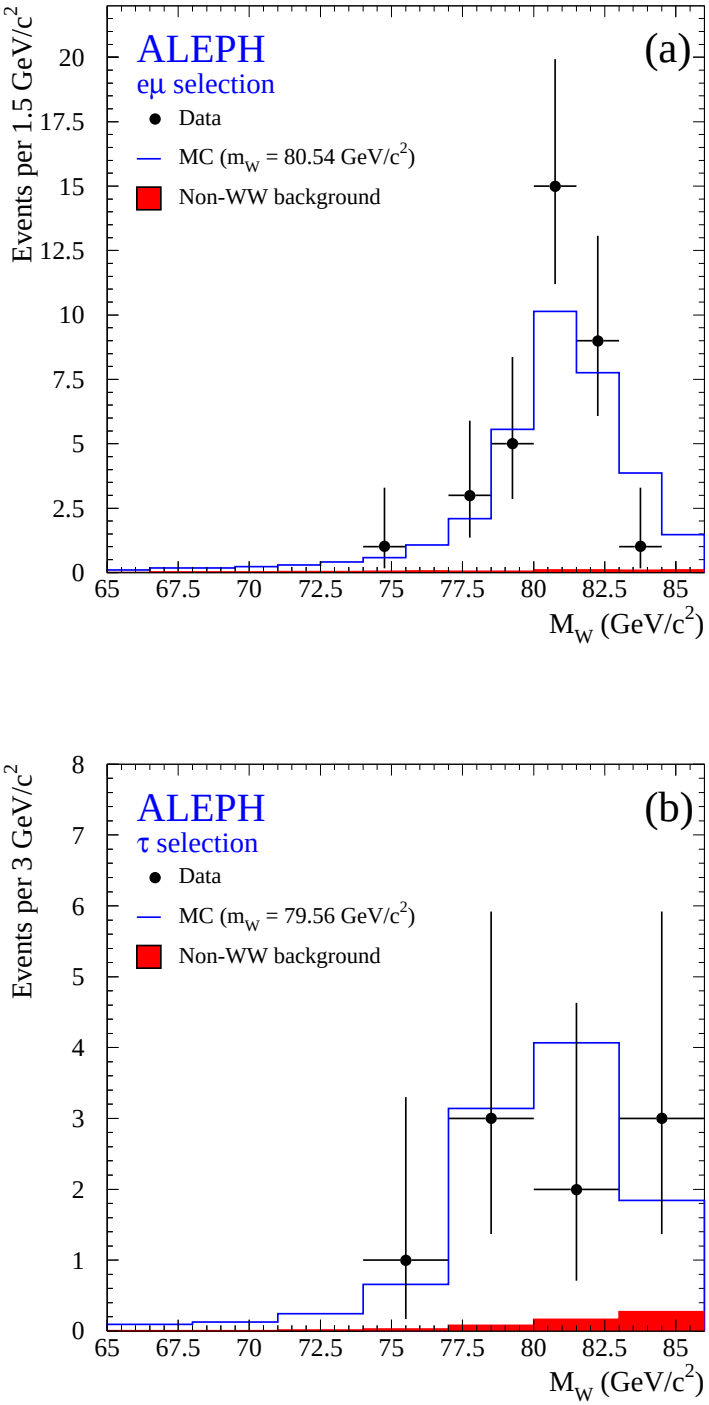

Figure 2: Mass distributions for eμ (a) and τ (b) data (points with error bars), background (shaded area) and signal+background Monte Carlo for the best fit to the data (solid line histogram).

7.1 Linearity of the reweighting technique

A critical test of the reweighting method is to ensure that the fitted mass agrees with the true input mass, when performing a fit to a Monte Carlo sample. The linearity of the fitted mass with the true input mass is studied for the hadronic, eμ and τ channels separately using the seven independent Monte Carlo samples with different input masses. For all channels, these distributions have slopes consistent with a value of one, and no

significant offsets are observed.

7.2 Event selection and mass range dependence

The hadronic events are selected by requiring the neural network output to be larger than -0.3. The stability of the result is studied as a function of this cut in Monte Carlo events. No statistically significant differences are observed in the fitted mass. By doing the same exercise with the data events, the same conclusion is reached. Similar studies are done for the semileptonic events, for which selections using event probabilities are applied. Again, no significant differences are observed.

The stability of the result as a function of the mass range used for the fit is checked for the three decay channels using both data and Monte Carlo samples. No significant mass range dependence is observed.

7.3 Mass measurement using a Breit-Wigner fit

As a cross-check of the reweighting method, simple relativistic Breit-Wigner functions are fitted to the observed invariant mass distributions of the three channels (4q, eμ and τ). In this method, the distortions described in Section 6.1 introduce a bias in the fitted mass which must be corrected for. The bias is found to be a linear function of the true input mass and is determined by fitting a straight line to the fitted mass versus the true mass, using the seven Monte Carlo samples generated with different m_{W} values. The straight line function is known as the *calibration curve*.

For the 4q channel, the expected error for a sample the size of the data is 0.45 GeV/c^2 before calibration and the correlation between the two mass estimators is $(47.1 \pm 4.2)\%$. The calibration curve obtained is given by $m_{4\mathrm{q}} = (80.68 \pm 0.02) + (0.73 \pm 0.04) \cdot (m_{\mathrm{W}}^{\mathrm{true}} - 80.25)$ (GeV/c^2); this function is used to correct both masses. After calibration, the expected error on the masses is 0.62 GeV/c^2 and the corrected values for the masses are $m_1 = 81.33 \pm 0.62$ GeV/c^2 and $m_2 = 81.17 \pm 0.62$ GeV/c^2. Combining the two masses with the expected correlation gives a final result for the W mass of:

$$4\mathrm{q}: \qquad m_{\mathrm{W}} = 81.25 \pm 0.53 \ \ \mathrm{GeV}/c^2,$$

which agrees with the result obtained with the reweighting technique.

For the eμ and τ channels, the expected errors before calibration are 0.43 GeV/c^2 for the eμ and 0.93 GeV/c^2 for the τ events. The calibration curves are given by $m_{\mathrm{e}\mu} = (80.77 \pm 0.02) + (0.87 \pm 0.02) \cdot (m_{\mathrm{W}}^{\mathrm{true}} - 80.25)$ (GeV/c^2) and $m_\tau = (81.00 \pm 0.03) + (0.73 \pm 0.04) \cdot (m_{\mathrm{W}}^{\mathrm{true}} - 80.25)$ (GeV/c^2). The expected errors on m_{W}, after calibration, are 0.49 GeV/c^2 and 1.28 GeV/c^2 for the eμ and τ events respectively. The corrected mass values are:

$$\begin{aligned} \mathrm{e}\mu: &\qquad m_{\mathrm{W}} = 80.52 \pm 0.49 \ \ \mathrm{GeV}/c^2 \\ \tau: &\qquad m_{\mathrm{W}} = 80.79 \pm 1.28 \ \ \mathrm{GeV}/c^2, \end{aligned}$$

also in agreement with the results obtained with the reweighting technique. For the τ data result, the mass difference between the Breit-Wigner and the reweighted results is studied using Monte Carlo subsamples. The probability of obtaining a difference larger than the observed one is 14%.

8 Systematic uncertainties

The systematic uncertainties on the W mass measurement are described in the following sections. They are summarised in Table 2.

8.1 Finite reference Monte Carlo statistics

The finite number of Monte Carlo events used as a reference in the reweighting method contributes a systematic uncertainty. A procedure is used where the reference sample is divided into smaller samples of equal size. Each of these samples are then fitted to the same data. The RMS of the fitted masses scales as the square root of the number of samples that the reference is divided into. From this method, the systematic error coming from Monte Carlo statistics is estimated to be $\Delta m_{\mathrm{W}} = 30, 35$ and 90 MeV/c^2 for the 4q, eμ and τ channels respectively.

8.2 Monte Carlo fragmentation parameters

The main fragmentation parameters in JETSET (Λ, M_{min}, σ, B and baryon production) are varied independently to extreme values, typically four standard deviations from their measured values [30]. With each variation, a new reference sample is made. The effect of these variations on the fitted mass is $\leq$ 10 MeV/c^2 for all the channels studied.

8.3 Diagrams in Monte Carlo reference

The matrix element used in this analysis corresponds to the CC03 diagrams instead of the complete matrix element which corresponds to all possible diagrams producing four fermions in the final state. The effect of this approximation is studied by comparing the weights derived from the CC03 matrix element with those derived from the complete matrix element as given by EXCALIBUR [18]. The contribution of the non-CC03 diagrams after the event selection is negligible. Using the four-fermion matrix element to weight the Monte Carlo events, the fitted mass from the data differs from the original one by 3 MeV/c^2.

8.4 Selection efficiency

The selection efficiencies are varied by $\pm 2\sigma$ of their statistical uncertainty, where σ=0.20, 0.13, 0.77% for the 4q, eμ and τ channels respectively. In addition, the mass dependence of the selection efficiencies are studied over a 2 GeV/c^2 mass range using the seven Monte Carlo samples with different m_{W} values, where maximal differences of 1.7$\pm$0.9%, 0.8$\pm$0.6% and 0.4$\pm$0.2% are observed for the 4q, eμ and τ selection efficiencies respectively. A linear dependence as a function of mass is implemented in the fit, with the slope obtained from the above studies. Both variations have a negligible effect on the fitted results.

8.5 Background contamination

For the hadronic events, the expected background remaining after the selection is about 20% of the sample. The small size of the data sample does not allow a detailed comparison

of its properties with the ones predicted by the Monte Carlo samples used. To overcome this problem, a technique using Z peak data was developed to evaluate the systematic uncertainty coming from the background estimation. High statistics Z peak data taken in 1994 are compared to $q\bar{q}$ Monte Carlo to evaluate the effect of any discrepancies in the background shape and normalisation. Selections similar to the preselections of this analysis, but scaled down according to beam energy, are applied to Z peak data. The observed disagreements at LEP1 energies are then applied as correction factors to the expected background in the 172 GeV analysis. The resulting observed shifts in the extracted W mass are then evaluated, and the largest mass shifts are taken as the systematic uncertainty due to the deficient modelling of the background. For the hadronic channel, the evaluated systematic uncertainty is $\Delta m_{\mathrm{W}} \leq 20$ MeV/c^2.

For the semileptonic events, the error from this source is expected to be small because the total background is only a small fraction of the signal. The error due to the background shape is estimated using data from LEP1, in a similar way as for the the hadronic channel. The uncertainty in the background normalisation is estimated by comparing the number of data and expected Monte Carlo events with an electron or muon probability less than 0.1. The resulting error from both sources is negligible.

8.6 Detector calibration

Studies indicate there are differences between data and Monte Carlo in the energy calibrations of the electromagnetic (ECAL) and hadronic (HCAL) calorimeters of up to 1.5% and 4% respectively. The effect of these discrepancies is estimated by globally rescaling the ECAL energy by $\pm 1.5\%$ and the HCAL energy by $\pm 4\%$ at the event reconstruction level and determining the change this produces in the W mass. Using the biggest change in both cases, the ECAL and HCAL errors are combined in quadrature to give the final errors: 56, 47 and 187 MeV/c^2 for the 4q, eμ and τ channels respectively.

8.7 Jet corrections in the kinematic fit

In studies of two-jet decays of the Z, the jet energy scale corrections described in Section 5.2 differ for data and Monte Carlo by up to 30% in the region $|\cos\theta_j| \geq 0.95$ where θ_j is the angle between the jet direction and the beam axis. A systematic error is evaluated by changing the corrections applied to the jet energy and angles by 30% of their values in a correlated way. Fitting to the data, systematic errors of $40, 90$ and 94 MeV/c^2 are obtained for the 4q, eμ and τ channels respectively.

8.8 W boson width variation

The value of the W mass obtained from the fit is studied as a function of the W width. The width is varied about its central value by the known experimental error $\pm\sigma = 0.07$ GeV [31]. The difference in the fitted mass is at most 10 MeV/c^2 for all the studied channels. A systematic uncertainty of 10 MeV/c^2 due to the uncertainty on the W width is quoted.

Table 2: Summary of the correlated and uncorrelated systematic errors on m_{W}.

	Δm_{W} (MeV/c^2)		
Source	4q	eμ	τ
Correlated errors			
MC Fragmentation	10	10	10
Reference MC diagrams	3	3	3
Detector calibration	56	47	187
Jet corrections	40	90	94
W width	10	10	10
Initial State Radiation	15	15	15
LEP Energy	30	30	30
Uncorrelated errors			
Reference MC Statistics	30	35	90
Background contamination	20	-	-
Colour reconnection	50	-	-
Bose-Einstein effects	40	-	-
Total	107	113	231

8.9 Initial state radiation

KORALW [9], the main event generator used in the studies, features QED initial state radiation up to $\mathcal{O}(\alpha^2 L^2)$, i.e. up to second order in the leading-log approximation. The effect of the missing terms on the W mass measurement is studied at generator level in [32] by degrading KORALW to $\mathcal{O}(\alpha^1 L^1)$ and checking the size of the pure $\mathcal{O}(\alpha^2 L^2)$ correction. A systematic effect on the W mass of 15 MeV/c^2 is quoted. The effect of the degradation of KORALW is also checked while properly taking into account detector effects. The differences observed are smaller than 15 MeV/c^2. A systematic error of $\Delta m_{\mathrm{W}} = 15$ MeV/c^2 from ISR is assigned.

8.10 LEP energy

The relative uncertainty on the LEP energy translates into the same relative uncertainty on the fitted mass, since the beam energy is directly used in the kinematic fit. For the quoted LEP beam energy uncertainty of $\Delta E_b = 30$ MeV [6], a systematic uncertainty of $\Delta m_{\mathrm{W}} = 30$ MeV/c^2 is assigned to all the channels.

8.11 Colour reconnection and Bose-Einstein effects

In hadronic events, the possible existence of colour reconnection and Bose-Einstein correlation effects between the two W's is pointed out as a source of systematic error on the W mass determination [16, 33, 34, 35], some of which quote large uncertainties. However, their size is likely to be sensitive to the topology of the selected events and to the actual procedure used to extract the W mass. The colour reconnection effect is studied using two Monte Carlo samples generated with EXCALIBUR, one with a colour

reconnection implementation, following the ansatz of [16], and the other without. The hadronic events of both samples are identical at the parton level. These are used as data, and the KORALW Monte Carlo sample with $m_{\mathrm{W}} = 80.25$ GeV/c^2 is used as a reference to fit the W mass. A difference of 20 ± 50 MeV/c^2 is observed between the fitted masses extracted from the data samples with and without colour reconnection.

To determine the effect of the Bose-Einstein (BE) correlation on the W mass measurement, the weighting method described in [32] is implemented using a KORALW Monte Carlo sample. The reference sample with $m_{\mathrm{W}} = 80.25$ GeV/c^2 is then fitted to this weighted Monte Carlo sample. A difference of 26 ± 40 MeV/c^2 is observed between this fitted mass and that obtained when no BE effect is included.

For both the colour reconnection and BE effects, the systematic error quoted is the statistical uncertainty of the estimated difference rather than the specific value of the difference observed.

9 Summary and conclusions

A Monte Carlo reweighting technique is used to measure the mass of the W boson. It is based on the direct comparison of the data mass distributions with those from the Monte Carlo weighted events.

Fully hadronic W decays are selected using a neural network method, while the semileptonic decays are identified using two separate selections: one for the $e(\mu)\nu q\bar{q}$ events and one for the $\tau\nu q\bar{q}$ events. The mass variables are determined in a four-constraint fit with rescaling for the 4q channel, and a two-constraint fit for the semileptonic channels. The resulting invariant mass distributions are compared with reweighted Monte Carlo events, and the values of the W mass are extracted in a binned log-likelihood fit. The following results are obtained:

$$\begin{aligned}
\mathrm{WW} \to q\bar{q}q\bar{q} \qquad & m_{\mathrm{W}} = 81.30 \pm 0.47(\mathrm{stat.}) \pm 0.11(\mathrm{syst.})\ \mathrm{GeV}/c^2, \\
\mathrm{WW} \to \ell\nu q\bar{q}\ (\ell = \mathrm{e}, \mu) \qquad & m_{\mathrm{W}} = 80.54 \pm 0.47(\mathrm{stat.}) \pm 0.11(\mathrm{syst.})\ \mathrm{GeV}/c^2, \\
\mathrm{WW} \to \tau\nu q\bar{q} \qquad & m_{\mathrm{W}} = 79.56 \pm 1.08(\mathrm{stat.}) \pm 0.23(\mathrm{syst.})\ \mathrm{GeV}/c^2,
\end{aligned}$$

where the statistical errors are the expected errors for Monte Carlo samples of the same integrated luminosity as the data. The average result for the semileptonic channels is: $m_{\mathrm{W}} = 80.38 \pm 0.43(\mathrm{stat.}) \pm 0.13(\mathrm{syst.})$ GeV/c^2. The correlated and uncorrelated systematic errors are combined using the statistical error weights. Combining all channels, with $\chi^2/ndf = 2.6/2$, the average W mass is:

$$m_{\mathrm{W}} = 80.80 \pm 0.32(\mathrm{stat.}) \pm 0.10(\mathrm{exp.syst.}) \pm 0.03(\mathrm{th.syst.}) \pm 0.03(\mathrm{LEP})\ \ \mathrm{GeV}/c^2,$$

where the theoretical systematic is due to ISR, Bose-Einstein and colour reconnection uncertainties and the last error is due to the LEP energy uncertainty. This result is consistent with the ALEPH result from the combined study of the cross section at threshold [1] and at 172 GeV [27]: $m_{\mathrm{W}} = 80.20 \pm 0.33(\mathrm{stat.}) \pm 0.09(\mathrm{syst.}) \pm 0.03(\mathrm{LEP})$ GeV/c^2. Combining the cross section measurements with the direct reconstruction measurement of this letter, the result is: $m_{\mathrm{W}} = 80.51 \pm 0.23(\mathrm{stat.}) \pm 0.08(\mathrm{syst.})$ GeV/c^2.

The W mass as measured in this letter is in agreement with direct determinations at $\mathrm{p\bar{p}}$ colliders [3] and at LEP both at 161 GeV [1, 2] and 172 GeV [36] centre-of-mass energies. It is also consistent with expectations based on precise measurements [37] obtained at the Z peak and elsewhere, assuming the validity of the minimal Standard Model.

Acknowledgments

It is a pleasure to congratulate our colleagues from the CERN accelerator divisions for the successful commissioning of the superconducting accelerating system and start-up of LEP2. We are indebted to the engineers and technicians in all our institutions for their contributions to the excellent performance of ALEPH. Those of us from non-member countries thank CERN for its hospitality.

References

[1] ALEPH Collaboration, *Measurement of the W mass in* $\mathrm{e^+e^-}$ *collisions at production threshold*, Phys. Lett. B401 (1997) 347.

[2] DELPHI Collaboration, *Measurement and interpretation of the W-pair cross section in* $\mathrm{e^+e^-}$ *interactions at 161 GeV*, Phys. Lett. B397 (1997) 158; L3 Collaboration, *Pair-Production of W Bosons in* $\mathrm{e^+e^-}$ *interactions at* $\sqrt{s} = 161$ *GeV*, Phys. Lett. B398 (1997) 223; OPAL Collaboration, *Measurement of the mass of the W boson in* $\mathrm{e^+e^-}$ *collisions at* $\sqrt{s} = 161$ *GeV*, Phys. Lett. B389 (1996) 416.

[3] UA2 Collaboration, *An improved determination of the ratio of W and Z masses at the CERN* $\mathrm{p\bar{p}}$ *collider*, Phys. Lett. B276 (1992) 354; CDF Collaboration, *A measurement of the W boson mass*, Phys. Rev. Lett. 65 (1990) 2243; Phys. Rev. D43 (1991) 2070; Phys. Rev. Lett. 75 (1995) 11; Phys. Rev. D52 (1995) 4784; DØ Collaboration, *Measurement of the W boson mass*, Phys. Rev. Lett. 77 (1996) 3309.

[4] Y. K. Kim, Lepton-Photon Conference Hamburg 1997, to appear in the proceedings.

[5] J. Lys (CDF Collaboration), Proceedings ICHEP '96, Warsaw; DØ Collaboration, *Direct measurement of the top quark mass*, Phys. Rev. Lett. 79 (1997) 1197; Average presented by P. Tipton, Proceedings ICHEP '96, Warsaw.

[6] The working group on LEP energy, *LEP Energy Calibration in 1996*, LEP Energy Group/97-01.

[7] ALEPH Collaboration, *ALEPH: A detector for electron-positron annihilations at LEP*, Nucl. Inst. Meth. A 294 (1990) 121.

[8] ALEPH Collaboration, *Performance of the ALEPH detector at LEP*, Nucl. Inst. Meth. A 360 (1995) 481.

[9] M. Skrzypek, S. Jadach, W. Placzek and Z. Wąs, Comp. Phys. Commun. 94 (1996) 216.

[10] M. Skrzypek et al., Phys. Lett. B372 (1996) 289.

[11] E. Barberio and Z. Wąs, Comp. Phys. Commun. 79 (1994) 291.

[12] V.S. Fadin, V.A. Khoze, A.D. Martin and A. Chapovsky, Durham report DTP/94/116.

[13] GRACE Manual, MINAMI-TATEYA group, KEK report 92-19 (1993).

[14] T. Sjöstrand, Comp. Phys. Commun. 82 (1994) 74.

[15] Working Group on QCD Event Generators, in "Physics at LEP2", CERN 96-01 (1996), vol. 2, 103.

[16] T. Sjöstrand and V.A. Khoze, Z. Phys. C62 (1994) 281.

[17] G. Gustafson, U. Pettersson and P.M. Zerwas, Phys. Lett. B209 (1988) 90; T. Sjöstrand and V.A. Khoze, Phys. Rev. Lett. 72 (1994) 28; L. Lönnbald and T. Sjöstrand, Phys. Lett. B351 (1995) 293; Working group on the W mass, in "Physics at LEP2", CERN 96-01 (1996), vol. 1, 190.

[18] F.A. Berends, R. Pittau and R. Kleiss, Comp. Phys. Commun. 85 (1995) 437.

[19] F.A. Berends, G. Burgers and W.L. Van Neerven, Phys. Lett. B185 (1987) 395; Nucl. Phys. B297 (1988) 429; Nucl. Phys. B304 (1988) 921.

[20] ALEPH Collaboration, *An experimental study of* $\gamma\gamma \to$ *hadrons at LEP*, Phys. Lett. B313 (1993) 509.

[21] S. Jadach, B.F.L. Ward, Z. Wąs, Comp. Phys. Commun. 79 (1994) 503.

[22] H. Anlauf et al., Comp. Phys. Commun. 79 (1994) 466.

[23] J.M. Hilgart, R. Kleiss and F. Le Diberder, Comp. Phys. Commun. 75 (1993) 191.

[24] JADE Collaboration, *Experimental studies on multi-jet production in* e^+e^- *annihilation at PETRA energies*, Z. Phys. C33 (1986) 23.

[25] ALEPH Collaboration, *Measurement of triple gauge-boson couplings at 172 GeV*, to be submitted to Phys. Lett. B.

[26] ALEPH Collaboration, *Updated measurement of the tau lepton lifetime*, CERN PPE/97-090, submitted to Phys. Lett. B.

[27] ALEPH Collaboration, *Measurement of W-pair cross section in* e^+e^- *collisions at 172 GeV*, CERN-PPE/97-102, submitted to Phys. Lett. B.

[28] Y.L. Dokshitser, Workshop on jets at LEP and HERA, Durham, 1990; S. Catani, Y.L. Dokshitser, M. Olsson, G. Turnock and B.R. Webber, Phys. Lett. B269 (1991) 432; N. Brown and W.J. Stirling, Z. Phys. C53 (1992) 629.

[29] Working group on WW cross sections and distributions, in "Physics at LEP2", CERN 96-01 (1996), vol. 1, 79.

[30] ALEPH Collaboration, *Studies of Quantum Chromodynamics with the ALEPH detector*, CERN-PPE/96-186, submitted to Physics Reports.

[31] R.M. Barnett et al., Phys. Rev. D54 (1996) 1.

[32] S. Jadach and K. Zalewski, CERN-TH/97-29 (1997).

[33] G. Gustafson, U. Pettersson and P. Zerwas, Phys. Lett. B209 (1988) 90.

[34] T. Sjöstrand and V. A. Khoze, Phys. Rev. Lett. 72 (1994) 28.

[35] J. Ellis and K. Geiger, CERN-TH/97-046, submitted to Phys. Lett. B.

[36] L3 Collaboration, *Measurements of mass, width and gauge couplings of the W Boson at LEP*, Phys. Lett. B413 (1997) 176; OPAL Collaboration, *Measurement of the W boson mass and W^+W^- production and decay properties in* e^+e^- *collisions at* $\sqrt{s}$*=172 GeV*, CERN-PPE/97-116 (1997), submitted to Zeit. für Phys. C.

[37] D.Ward, EPS '97 in Jerusalem, to appear in the proceedings.